

# Thermal and chemical properties of $\text{TiO}_2$ – $\text{SiO}_2$ porous glass–ceramics

TOSHINORI KOKUBU, MASAYUKI YAMANE\*

*Department of Industrial Chemistry, Miyakonojo National College of Technology, Yoshio-cho, Miyakonojo, Miyazaki 885, Japan and \*Department of Inorganic Materials, Tokyo Institute of Technology, Ookayama, Meguro-ku, Tokyo 152, Japan*

The thermal and chemical stability of porous glass–ceramics of the  $\text{TiO}_2$ – $\text{SiO}_2$  system have been investigated. Porous glass–ceramics containing both anatase and rutile had thermal expansion coefficients of  $40$  to  $55 \times 10^{-7} \text{ K}^{-1}$  in the range  $0$  to  $700^\circ \text{C}$ . They remained porous up to  $1000^\circ \text{C}$ , while the pores of high-silica porous glass of Vycor type collapsed completely at that temperature. The high thermal stability of the porous glass–ceramics may be attributed to a high viscosity due to dispersed crystallites of anatase and rutile in the skeleton. Most of the anatase in the skeleton was transformed to rutile by heat treatment at  $900^\circ \text{C}$ , but some of it remained untransformed even after 6 h. Surface  $-\text{OH}$  groups identified by IR spectroscopy were removed by dehydration polycondensation with heating up to  $900^\circ \text{C}$ . The porous glass–ceramics were quite durable to alkali solution compared with high-silica porous glass. The excellent durability of these porous glass–ceramics was attributed to the large amount of  $\text{TiO}_2$  contained in the skeletal structure.

## 1. Introduction

Recently we reported the preparation of porous glass–ceramics of high titania content from glasses of the  $\text{TiO}_2$ – $\text{SiO}_2$ – $\text{Al}_2\text{O}_3$ – $\text{B}_2\text{O}_3$ – $\text{CaO}$ – $\text{MgO}$  system by the same process as the conventional porous glass fabrication from borosilicate glass [1]. The prepared porous glass–ceramics were composed mainly of  $\text{TiO}_2$  and  $\text{SiO}_2$  which remained undissolved after the leaching of the  $\text{Al}_2\text{O}_3$ – $\text{B}_2\text{O}_3$ – $\text{CaO}$ -rich phase with hot HCl solution. They contained a large amount of anatase and rutile in their skeleton and had a high surface area of  $100$  to  $400 \text{ m}^2 \text{ g}^{-1}$  for a pore volume of about  $0.4 \text{ ml g}^{-1}$ . Their mean pore diameter could be controlled within the range from  $1$  to  $20 \text{ nm}$  by varying the composition of the mother glass and the temperature and time of the heat treatment for phase separation.

In order to apply these porous glass–ceramics in various fields such as supports for catalysts, photocatalysts [2–8], gas sensors [9–12] and so on [13–21], it is necessary to know the thermal and chemical stability of the material under use.

When the material is used as a catalyst support for high-temperature reactions, for example, a high specific surface area under high temperature, as well as high mechanical strength, is essential. When the material is used as a collector of uranium from sea-water, on the other hand, the chemical durability is the most important property.

This paper reports the thermal and chemical stability of  $\text{TiO}_2$ -containing glass–ceramics investigated by means of dilatometry, X-ray diffraction, IR spectroscopy, specific surface area measurement and durability tests in alkali solution.

## 2. Experimental procedure

### 2.1. Sample glass–ceramics

Experiments were carried out on four kinds of glass–ceramics whose compositions are shown in Table I along with the compositions of the original glasses. Samples 1A and 1B were prepared from the original glass of the same composition whose crystallization behaviour was described in the previous report. Samples 1A, 1B and 2 were platelets of about  $0.5 \text{ mm}$  thickness. Sample No. 3 was powdery.

These samples were obtained by leaching  $\text{Al}_2\text{O}_3$ – $\text{B}_2\text{O}_3$ – $\text{CaO}$ -rich phase from phase-separated glasses with  $0.5 \text{ N HCl}$  at  $90^\circ \text{C}$  for  $24 \text{ h}$ , which was mild enough to prevent cracking during treatment.

The specific surface area, pore volume and mean pore radius of the samples are shown in Table II along with the conditions of heat treatment for phase separation. Sample No. 1A, which had a density of  $3.15 \text{ g cm}^{-3}$ , contains a larger amount of anatase than Sample No. 1B. Sample No. 2 has a similar composition to No. 1A but contains a larger amount of crystallite than the latter.

Experiments were also carried out on two kinds of  $\text{TiO}_2$ -free porous glasses employed as reference materials. One was controlled-pore glass (CPG) (Electro-Nucleonic, Inc., Fairfield, New Jersey, USA) having a surface area of  $150 \text{ m}^2 \text{ g}^{-1}$ . The other was high-silica porous glass (HSPG) prepared by the present author. HSPG contained  $98.0 \text{ mol } \% \text{ SiO}_2$  and had a surface area of  $180 \text{ m}^2 \text{ g}^{-1}$ .

### 2.2. Thermal stability

Changes in structure and properties with heat treatment were investigated by means of linear shrinkage

TABLE I Chemical compositions of porous glass-ceramics and their mother glasses\*

Sample No.	Composition (mol %)					
	TiO <sub>2</sub>	SiO <sub>2</sub>	Al <sub>2</sub> O <sub>3</sub>	B <sub>2</sub> O <sub>3</sub>	CaO	MgO
1A	50.6	47.8	1.0	0.2	0.4	0.1
1B	57.5 (25.0)	41.2 (31.0)	0.8 (12.5)	0.0 (7.5)	0.4 (22.5)	0.1 (1.5)
2	49.7 (18.0)	48.7 (38.0)	0.7 (12.5)	0.0 (7.5)	0.7 (22.5)	0.1 (1.5)
3	37.5 (17.0)	62.4 (34.0)	0.1 (13.0)	0.0 (7.0)	0.0 (24.0)	0.0 (5.0)

\*Numbers in parenthesis represent the nominal composition of the mother glass.

measurements and surface area measurements, and IR spectroscopy and X-ray diffraction measurements were made on Sample No. 1A.

The linear shrinkage of the glass-ceramics was measured with a Rigaku TMA 8121-S thermomechanical analyser on platelet samples: for No. 1A of size 0.5 mm × 5.0 mm × 15.12 mm, for No. 1B of 0.5 mm × 5.0 mm × 19.46 mm, for No. 2 of 0.5 mm × 5.0 mm × 17.29 mm and for HSPG of 0.5 mm × 5.0 mm × 17.79 mm, at a heating rate of 10 K min<sup>-1</sup> within the range 40 to 800°C. After the first run up to 800°C, the samples were again heated up to 800°C at the same rate in order to obtain the thermal expansion coefficient.

IR absorption spectroscopy was carried out with a Jasco A-302 infrared spectrophotometer on three platelet samples which had been subjected to heat treatment for 12 h at 400, 700 and 900°C. These temperatures correspond to the respective inflection points in the first and second TMA measurements. A heating period of 12 h is optimal to obtain a good spectrum.

X-ray diffraction measurement was carried out with a Shimadzu XD-5A diffractometer using nickel-filtered CuK $\alpha$  radiation of 30 kV, 20 mA on three specimens of No. 1A isothermally heated at the same temperatures as the samples for IR spectroscopy, i.e. 400, 700 and 900°C, for 6 h.

Thermal stability was also examined by measuring the surface area of the pulverized samples after isothermal treatment for 12 h at various temperatures between 600 and 1200°C.

### 2.3. Measurement of chemical durability

The durability of the porous glass-ceramics to alkaline solutions was determined by measuring the weight loss. 1 g of sample powder of size between 177 and 250  $\mu$ m was placed on a glass filter of G3 size (20 to 30  $\mu$ m opening) to be leached in 100 ml of 0.1 N NaOH solution at 40°C for up to 200 h. The decrease in weight at every 24 h was measured on the sample

powder after being immersed in 0.1 N HCl solution to neutralized NaOH, followed by washing with sufficient water on a G3 filter. The sample powder remaining on the filter was then dried out in a vacuum. The weight at each measurement was plotted against the leaching time.

## 3. Results

### 3.1. Change in structure and properties with heat treatment

Changes in sample size of Nos 1A, 1B, 2 and HSPG with linear-rate heating in the first and second run are shown in Figs 1 and 2.

All the samples studied shrank gradually with heating in the first run, but the degree of shrinkage of the porous glass-ceramics was much smaller than that of HSPG.

The porous glass-ceramics Nos 1A, 1B and 2 exhibited thermal expansion of the order of 40 to 55 × 10<sup>-7</sup> K<sup>-1</sup> in the second run, although HSPG remained unchanged until it shrank again at a temperature around 700°C.

The changes in the IR spectrum of porous glass-ceramics No. 1A with heat treatment are shown in Fig. 3. Strong absorption peaks around 3000 and 1620 cm<sup>-1</sup> are attributed to molecular water adsorbed on the micropore walls of the glass-ceramics. The sharp peak at 3750 cm<sup>-1</sup> is attributed to free hydroxyl [22]. It is clear from the figure that a significant amount of molecular water remains in the micropores up to 700°C. The water, however, is removed at 900°C as well as free hydroxyl.

X-ray diffraction patterns of the porous glass-ceramics after isothermal treatment at 400, 700 and 900°C are shown in Fig. 4. In the figure the peaks of anatase decreased slightly with increasing temperature and become very weak after soaking for 6 h at 900°C. It is clear that the anatase turned to rutile with increasing heat-treatment temperature.

Changes in the surface area of the porous glass-ceramics due to collapse of the pores are shown in

TABLE II Conditions of thermal treatment for phase separation and characteristics of the porous glass-ceramics

Sample No.	Thermal treatment		Surface area (m <sup>2</sup> g <sup>-1</sup> )	Pore volume (ml g <sup>-1</sup> )	Mean pore radius (nm)
	Temperature (°C)	Period (h)			
1A	760	15	167	0.36	4.35
1B	760	20	126	0.40	6.39
2	760	20	180	0.44	4.92
3	780	12	249	0.42	3.80

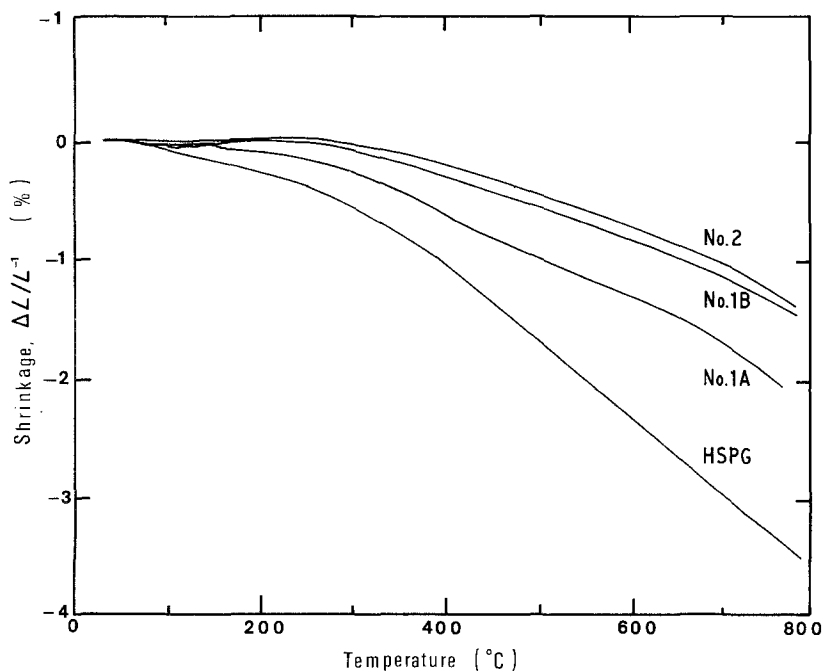


Figure 1 Linear shrinkage of platelets of porous glass-ceramics and HSPG under constant-rate heating at  $10 \text{ K min}^{-1}$ .

Fig. 5 along with data for the reference samples CPG and HSPG. Samples 1A and 3 were comparatively thermostable and stayed porous even at  $1000^\circ\text{C}$ , while the reference samples CPG and HSPG completely shrank to zero surface area at  $800$  and  $1000^\circ\text{C}$ , respectively.

### 3.2. Chemical properties of the porous glass-ceramics

The durabilities of porous glass-ceramics in alkaline solution are compared with those of CPG and HSPG in Fig. 6. The reference porous silicate glasses were very weak to alkaline solution and most of the powder passed through a G3 filter after 100 h leaching. The porous glass-ceramics, on the other hand, were quite durable and 50% of the initial weight remained on a G3 filter even after 200 h of leaching. The durability increased with increase of  $\text{TiO}_2$  content and with the deposition of rutile in the glass-ceramics.

## 4. Discussion

### 4.1. Thermal and mechanical properties

Linear shrinkage was observed for all samples in the first run. The curves for this shrinkage are similar to that observed for high-silicate porous glass prepared by the Vycor process [23], or silica gel obtained by the hydrolysis and polycondensation of silicon alkoxide [24]. In the case of silica gel, the shrinkage occurring in linear-rate heating is explained by three different mechanisms depending on the temperature [24].

The first shrinkage observed in the range up to about  $200^\circ\text{C}$  is attributed to an increase in surface energy due to the desorption of physically adsorbed water on the micropore wall. The shrinkage observed in the next range up to about  $550^\circ\text{C}$  is due to increased packing efficiency and skeletal densification. The third kind of shrinkage observed above  $550^\circ\text{C}$ , is due to viscous sintering to dissipate the surface energy.

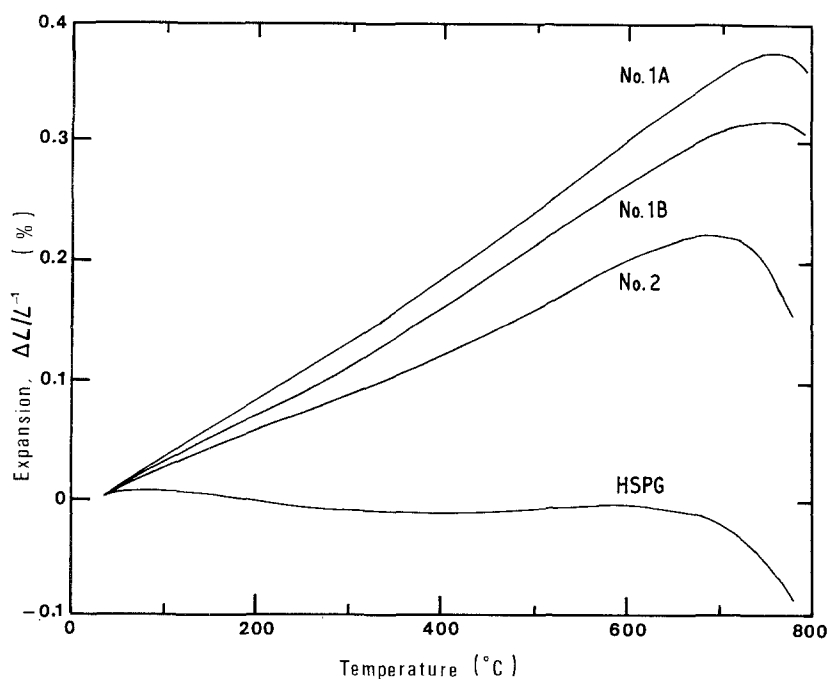


Figure 2 Thermal expansion of porous glass-ceramics in second run of constant-rate heating at  $10 \text{ K min}^{-1}$ .

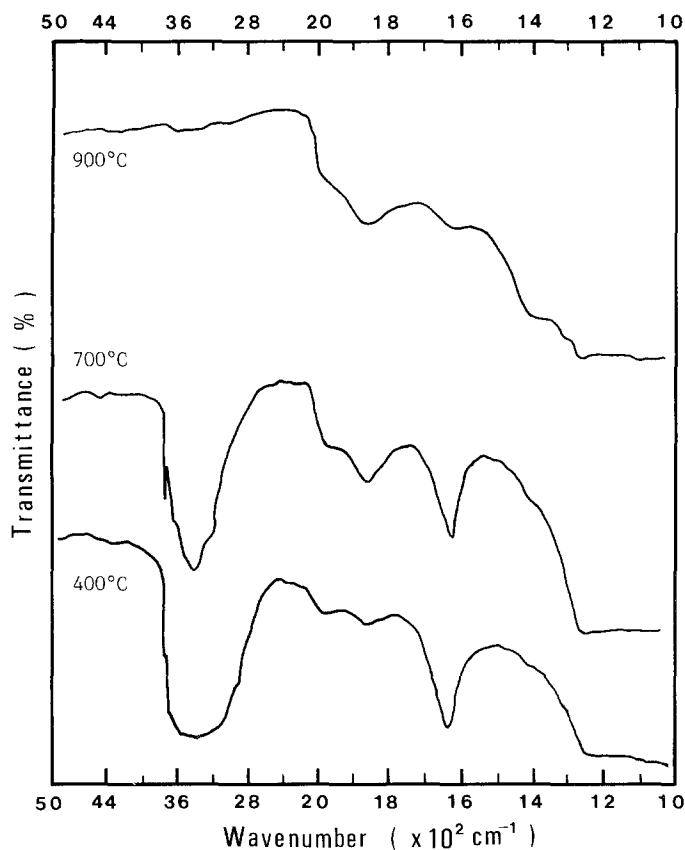


Figure 3 Changes in IR spectra of Sample No. 1A with heat treatment at 400, 700 and 900°C.

It is uncertain whether the second mechanism is applicable to the shrinkage of the glass-ceramics of the present study, but the first and third mechanisms are feasible.

The linear strain,  $\epsilon$ , caused by an increase in surface energy due to the desorption of physically adsorbed

water, is given by [24]

$$\epsilon = (1 - \nu)S\varrho_s\Delta\gamma/E$$

where  $S$  is surface area and  $\varrho_s$  skeletal density.  $\Delta\gamma$  the change in specific surface energy, and  $\nu$  and  $E$  are Poisson's ratio and Young's modulus, respectively.

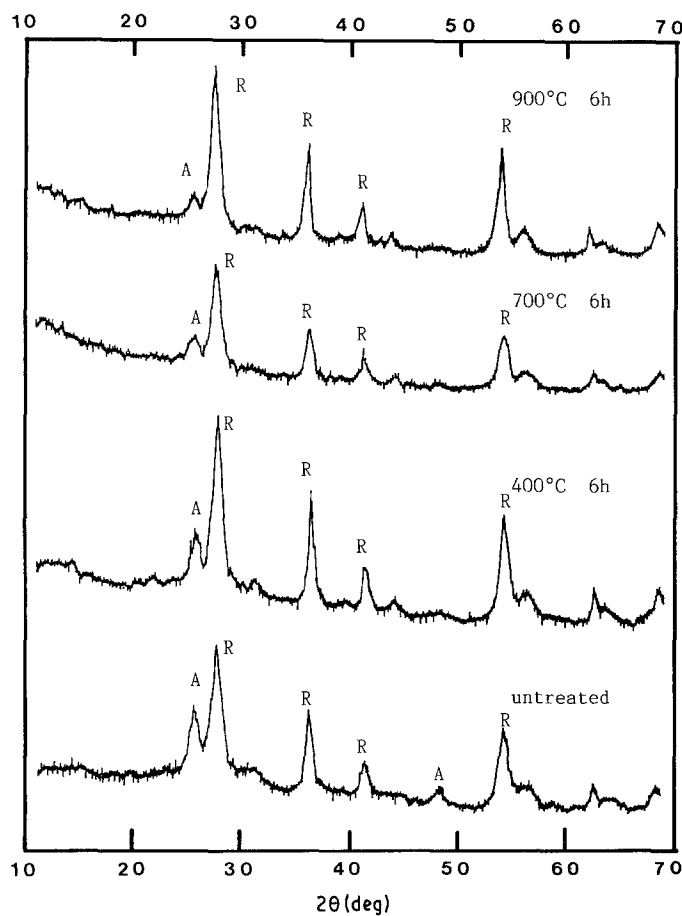


Figure 4 Changes in X-ray diffraction pattern of Sample No. 1A with heat treatment at 400, 700 and 900°C.

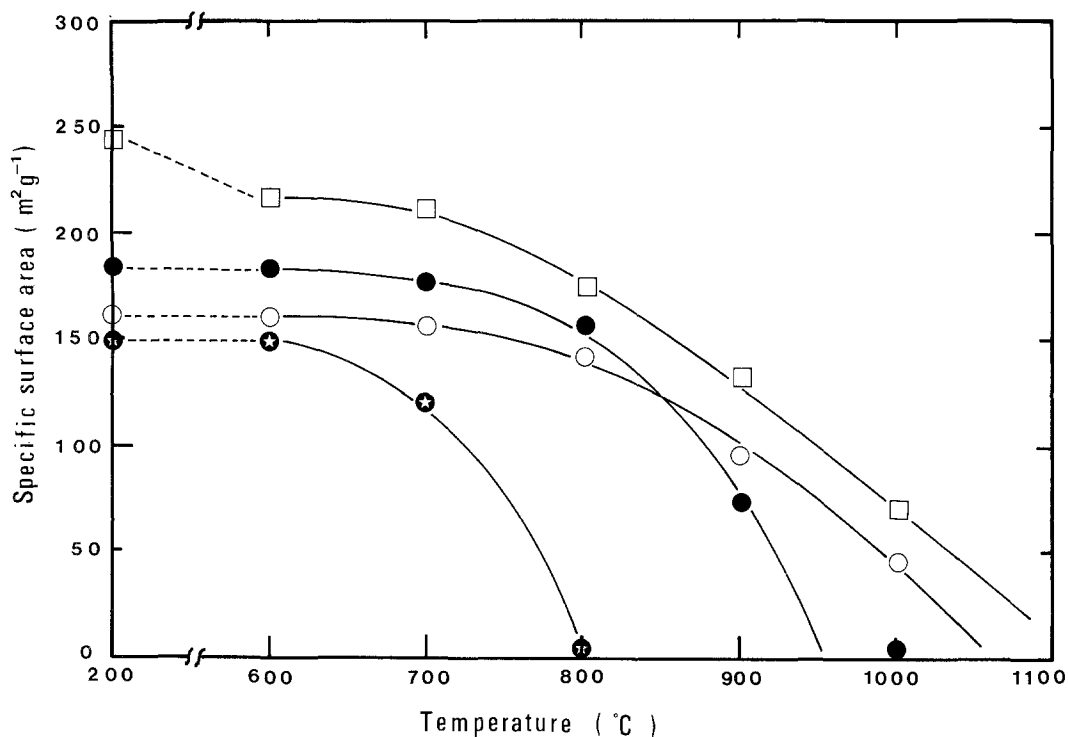


Figure 5 Changes in the specific surface area of porous glass-ceramics and reference samples with temperature: (○) No. 1A, (□) No. 3, (●) HSPG, (⊕) CPG.

The specific surface areas of Sample No. 1A and HSPG are comparable to each other. The skeletal density of the former is larger than that of the latter. Therefore, the small shrinkage of the porous glass-ceramics compared to that of HSPG may suggest that the values of Poisson's ratio and Young's modulus of the former are larger than those of the latter.

The curves in Fig. 2 represent the thermal behaviour of the porous glass-ceramics after the removal of adsorbed water. The thermal expansion coefficients of Nos 1A and 2 were  $53 \times 10^{-7}$  and  $39 \times 10^{-7} \text{ K}^{-1}$ , respectively, in the temperature range 0 to 700°C. This difference may be attributed to a difference in the

degree of crystallization between the samples. More important, however, is that these values of expansion coefficient are comparable to that of commercial thermostable glass, meaning that the porous glass-ceramics have a fairly good stability to thermal shock.

The linear shrinkage observed at a temperature around 800°C in the second run is due to viscous sintering. This agrees with the change in the specific surface area with heat treatment (Fig. 5). The smaller change in the specific surface area of porous glass-ceramics compared with HSPG is probably attributable to their high viscosity, which is important for the application of the material to high-temperature use.

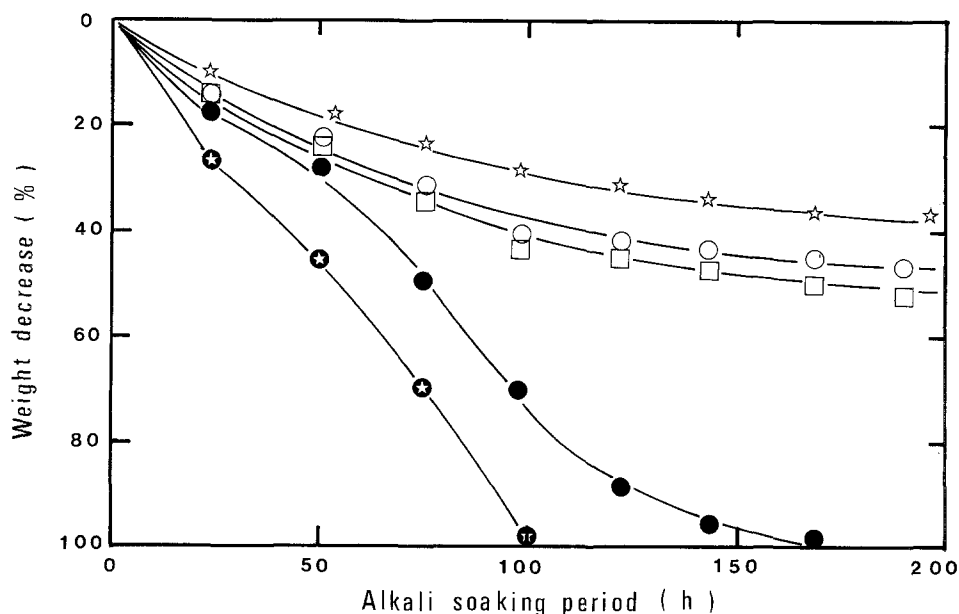


Figure 6 Decrease in weight of the samples soaked in alkaline solution of 0.1N NaOH at 40°C: (☆) No. 1B, (○) No. 1A, (□) No. 3, (●) HSPG, (⊕) CPG.

## 4.2. Structural stability at elevated temperature

According to the phase diagram of the Ti–TiO<sub>2</sub> system, anatase remains as a stable phase up to about 750°C [25]. The results for the X-ray analysis of Sample No. 1A, on the other hand, show that a trace of anatase is still remaining even after the treatment for 6 h at 900°C. This suggests that the transformation of anatase to rutile which accompanies the increase in volume was slightly hindered by the glassy phase of silica surrounding these crystallites. This is a desirable phenomenon for the application of the material to the field of photocatalysis.

Surface hydroxyl was removed by heat treatment at 900°C. This is similar to the reduction in hydroxyl during the densification of an alkoxy-derived silica gel in which the dehydration polycondensation of ≡SiOH groups occurs [24].

## 4.3. Durability to alkali solution

It is clear from Fig. 6 that the durability of the porous glass–ceramics to alkali solution is superior to that of HSPG which does not contain TiO<sub>2</sub>.

This phenomenon, which is highly desirable for the application of the material in an alkaline environment such as sea-water (pH = 8.0), may be explained by the very low solubility of TiO<sub>2</sub> in alkaline solution [26]. That is, when a small amount of TiO<sub>2</sub> is dissolved, the solution near the surface of the material is saturated with TiO<sub>2</sub>, and the further dissolution of TiO<sub>2</sub> is extremely hindered.

In summary, it may be emphasized that the TiO<sub>2</sub>-containing porous glass–ceramics developed by the authors can be used in a variety of fields owing to their high durability to alkaline solution and excellent thermal stability, giving a high specific surface area at high temperature.

## References

1. T. KOKUBU and M. YAMANE, *J. Mater. Sci.* **20** (1985) 4309.
2. A. FUJISHIMA and K. HONDA, *Nature* **238** (1972) 37.
3. L. KURUZYNSKI, H. D. GESSER, C. W. TURNER and E. A. SPEERS, *ibid.* **291** (1981) 399.
4. D. DUONGHONG, E. BORGARELLO and M. GRATZEL, *J. Amer. Chem. Soc.* **103** (1981) 4685.
5. M. GRATZEL, *Acc. Chem. Res.* **14** (1981) 376.
6. S. SATO and J. M. WHITE, *J. Catal.* **69** (1981) 128.
7. *Idem.*, *J. Phys. Chem.* **85** (1981) 592.
8. H. YONEYAMA, Y. TOMOGUCHI and H. TAMURA, *ibid.* **76** (1972) 3460.
9. T. Y. TIEN, H. L. STADLER, E. F. GIBBONS and P. J. ZACMANIDS, *Amer. Ceram. Soc. Bull.* **54** (1975) 280.
10. F. BOZON-VERDURAZ, A. OMAR, J. ESCARD and B. PONTVIANNE, *J. Catal.* **53** (1978) 126.
11. L. A. HARRIS, *J. Electrochem. Soc.* **127** (1980) 2657.
12. N. YAMAMOTO, S. TONOMURA, T. MATSUOKA and H. TONOMURA, *Surf. Sci.* **92** (1980) 402.
13. I. ASO, M. NAKAO, N. YAMAZOE and T. SEIYAMA, *J. Catal.* **57** (1979) 287.
14. M. A. VANNICE and R. L. GARTEN, *ibid.* **56** (1979) 236.
15. *Idem.*, *ibid.* **63** (1980) 255.
16. M. A. VANNICE and C. J. SUDHAKER, *J. Phys. Chem.* **88** (1984) 2429.
17. G. G. RAUPP and J. D. DUMESIC, *ibid.* **89** (1985) 5240.
18. F. E. LITTMAN and G. A. CROOPNIK, US Office Saline Water, Research Development Progress Report No. 720 (Washington, USA, 1971).
19. P. W. McMILLAN and C. E. MATTHEWS, *J. Mater. Sci.* **11** (1976) 1187.
20. A. MAKISHIMA and J. D. MACKENZIE, *Yogyo-Kyokai-shi* **83** (1975) 507.
21. N. OGATA, *Nippon-kaisui-gakkai-shi* **31** (1977) 97.
22. M. J. D. LOW and N. RAMASUBRAMANIAN, *J. Phys. Chem.* **70** (1966) 2740.
23. R. MADDISON and P. W. McMILLAN, *Glass Technol.* **21** (1980) 297.
24. C. J. BRINKER, G. W. SCHERER and E. P. ROTH, *J. Non-Cryst. Solids* **70** (1985) 301.
25. E. M. LEVIN, C. R. ROBBINS and H. F. MCMURDIE, *Phase Diagrams for Ceramists*, Vol. 1 (American Ceramic Society, Columbus, Ohio, USA, 1964) p. 41.
26. H. TAKAGI, T. KOKUBO and M. TASHIRO, *Yogyo-Kyokai-shi* **89** (1981) 418.

Received 29 August  
and accepted 21 November 1986